



ELSEVIER

Available online at www.sciencedirect.com

Journal of volcanology
and geothermal research

Journal of Volcanology and Geothermal Research xx (2007) xxx – xxx

www.elsevier.com/locate/jvolgeores

Non-linear explosion tremor at Sangay, Volcano, Ecuador

Jonathan M. Lees^{a,*}, Mario Ruiz^a *University of North Carolina, Department of Geological Sciences, CB#3315, Mitchell Hall, Chapel Hill, NC 27599-3315, United States*

Received 1 February 2007; accepted 6 August 2007

Abstract

A detailed analysis of discrete degassing pulses, chugs, at Sangay volcano, was performed on seismic and infrasonic records to determine the physics of the conduit. Infrasonic chugging signals appear as repetitive pulses with small variations in amplitude and time lag. An automated time-domain analysis was developed to measure with high precision time intervals and amplitudes at different wave arrivals, reducing the possibility error associated with hand picking. Using this automated method, a strong positive correlation of acoustic amplitude with repose time between individual pulses on chugging signals of Sangay was found on numerous oscillating sequences. Frequency gliding of apparent harmonic frequencies generally trends from high to low frequency at Sangay, in contrast to trends at Karymsky Volcano, Russia. A new description of chugging events using wavelet transform methods, appropriate for non-stationary signals, shows subtle changes in the waveforms relate to physical processes in the volcano. A system of non-linear feedback, based on choked flow at the vent, is postulated as the most likely source of this volcanic tremor. © 2007 Elsevier B.V. All rights reserved.

Keywords: volcanoes; explosions; Strombolian activity; infrasound; seismo-acoustic; non-linear; wavelet transform; harmonic tremor; quasi-periodic

1. Introduction

Volcanic “chugging”, a specialized tremor observed at several exploding volcanoes, is currently being used to understand the physics and structure of volcanic conduits during low level Strombolian style activity. Chugging has been identified most clearly at Arenal Volcano, Costa Rica, (Benoit and McNutt, 1997; Garces et al., 1998; Hagerty et al., 2000), and Karymsky Volcano, Kamchatka, (Johnson et al., 1998; Johnson and Lees, 2000; Lees et al., 2004) as a sequence of puffing or explosions following an initial explosion which apparently triggers

the sequence. The quasi-periodic chugging sequence consistently exhibits an inter-pulse period varying from 0.7–2 s and produces a series of pulses in the infrasonic frequency band. Chugging sequences are not restricted to the low frequency bands and can often be heard in audible frequency ranges, although we know of no documented cases of researchers visually observing gas or other emissions associated directly with chugging. This maybe due to the fact that chugging usually follows a larger Strombolian style explosion and pulsations that occur in the aftermath are obstructed by the larger amounts of gas and ash remaining from the initial blast. The individual infrasonic chugging signals appear to be discrete and time limited, often evolving over the length of the chugging sequence. Corresponding seismic signals, distorted because they are convolved with the intervening earth structure, display more complex signals

* Corresponding author. Tel.: +1 919 962 0695; fax: +1 919.

E-mail address: jonathan.lees@unc.edu (J.M. Lees).

URL: <http://www.unc.edu/~leesj> (J.M. Lees).

48 associated with path effect and site response, as well as
 49 the source time function of individual tremor pulses.
 50 Since the acoustic signals do not suffer significant
 51 distortion from path effects, we concentrate primarily on
 52 analysis of the infrasonic signals in this study.

53 From April 21–26, 1998, two portable, broadband,
 54 seismic stations including infrasonic microphones were
 55 deployed on the southern flanks of Sangay to monitor
 56 activity and record infrasonic acoustic waves as well as
 57 seismic emission from the vents (Fig. 1). During this
 58 survey, 38 chugging signals were recorded on seismic and
 59 acoustic stations. Johnson and Lees (2000) provide a

detailed description of the 1998 deployment and show that
 60 chugging events of Sangay and Karymsky have, in gen-
 61 eral, similar waveforms, although differences in occur-
 62 rence, duration and spectral content were cited. Prior to the
 63 1998 deployment, long-period, hybrid and tremor events
 64 (about 5/day) were recorded in 1995 on a short period
 65 seismic station 4.3 km from the summit. The 1995 events
 66 exhibited characteristics similar to the 1998 recordings.
 67 Some of the 1995 events were associated with audibly and
 68 visually observed explosions followed by roar-like,
 69 pulsating, rhythmic exhalations (GVN, 1996). Because
 70 of the remoteness of Sangay, the volcano is not monitored
 71

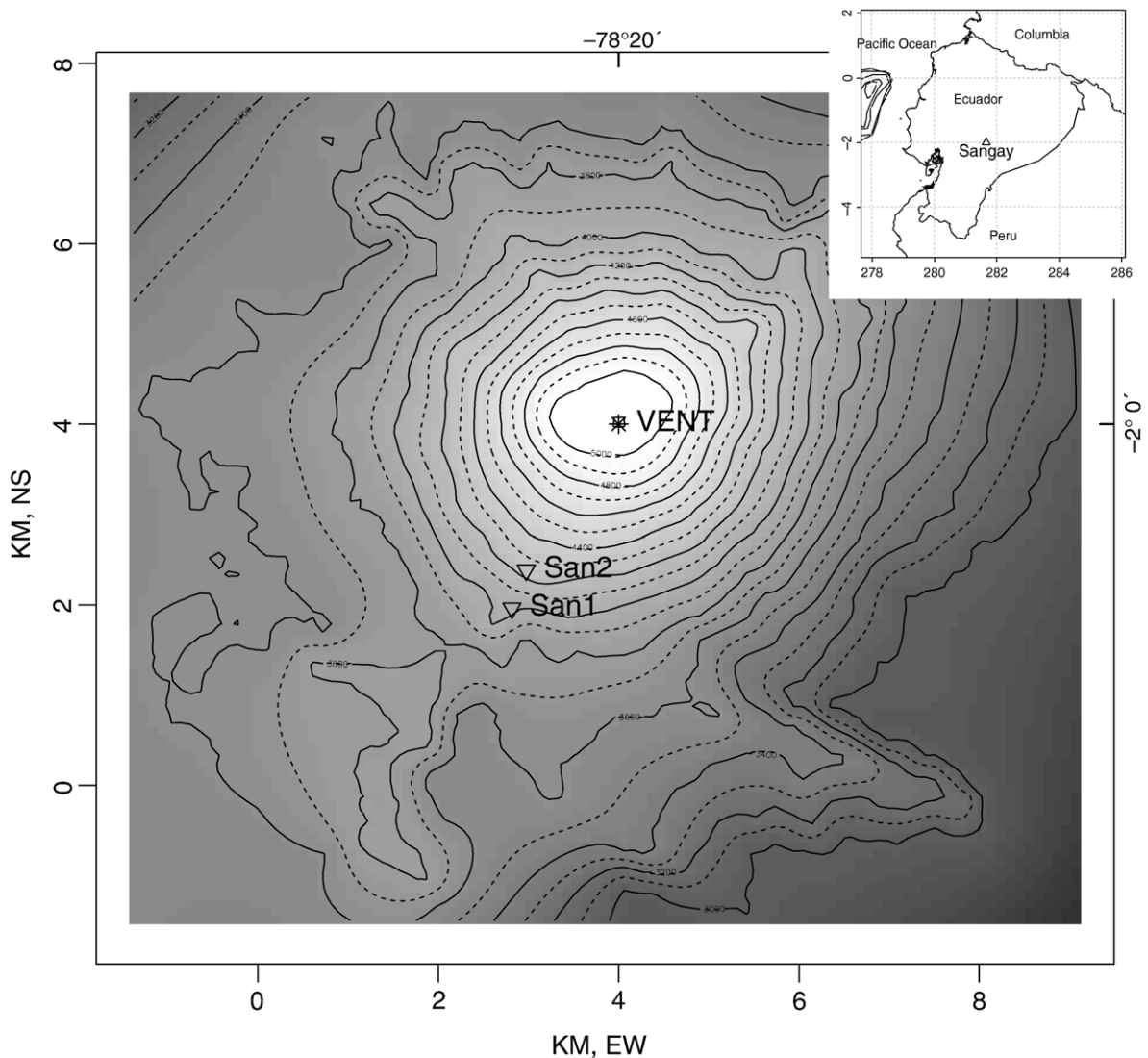


Fig. 1. Topographic map of Sangay showing station location and vent region. Contours are drawn at 200 m intervals. Stations were located down slope from the active vent. Data presented in this paper are from station San2 1200 m from the vent.

regularly, although we expect this low level activity, including pulsating tremor, is ongoing and persistent.

Sangay is the most active volcano in the Northern Andes. It has been in a state of continuous eruption for as long as historic accounts are available. Large eruptive activity, including high ash columns, has been reported on more than 16 occasions between 1728 and 1980 (J. Egred, pers. comm.). A detailed review of the geology, petrology and descriptions of the volcano can be found in Monzier et al. (1999). Ongoing activity at Sangay consists primarily of low level Strombolian explosions with block and ash explosions, occurring, on average, 1–2 times per hour. In the past few years activity has migrated across the vents at the summit. This paper uses data collected solely from the 1998 deployment.

At Sangay, the summit complex of vents contains several craters with a WSW–ENE trend, although at the time of the field experiment, only a crater at the NE edge was erupting. Time delays between acoustic and seismic arrivals have a mean value of 4.02 s ($\sigma=0.105$ s) at station SAN2, the closest to the vent. Based on the consistency of these time delays, we are confident that the sources studied here are derived from only one of the active vents. Onsets of acoustic and seismic waveforms of explosions recorded at Sangay are remarkably similar despite the emergent nature of seismic signals (Johnson and Lees, 2000). These observations support the hypothesis of repeatable sources at stable locations for this type of event at Sangay.

Of all volcanoes that exhibit “chugging” behavior Sangay and Karymsky share seismo-acoustic characteristics that are more similar to each other than others studied by the authors. It is worthwhile noting that these two volcanoes differ in their size and tectonic setting. Sangay vents are located at 5000 m elevation as compared to Karymsky’s 1600 height. Each volcano is conical in shape, located in a subduction zone setting, although Sangay is situated at the southern terminus of volcanism in the Northern Andes whereas Karymsky is far from potentially disturbing edge effects associated with slab termination. Each volcano exhibits an array of whole rock geochemistry ranging from silicic to mafic character, although for the most both volcanoes are dominated by andesitic eruptions and lava flows (Zobin and Levina, 1998; Monzier et al., 1999; Eichelberger and Izbekov, 2000; Ozerov et al., 2003; Lees et al., 2004).

Analysis in the earlier paper (Johnson and Lees, 2000) used spectrogram analysis of signals to show effects of harmonic tremor and gliding, the time-varying fluctuations of the fundamental mode and harmonics of chugging series. Although Sangay and Karymsky volcanoes share physical similarities in their eruption

activity parameters (eruptive scale time, magma viscosity, volatile content, and mass flux through the vent) chugging events at each exhibit broad differences in duration, occurrence, and frequency content. In this paper we extend the analyses described earlier and show that activity at Sangay is much more similar to Karymsky behavior than previously understood. Using an automatic time-domain analysis of amplitude–time lapse ratios, we show that chugging amplitudes recorded on infrasonic sensors appear to be correlated with time between individual chugs, as observed at Karymsky in 1997 (Lees et al., 2004). This observation has important implications for modeling volcanoes in general, regarding the interaction of vent and ascending combinations of mixed-phase mass prior to expulsion from the volcano orifice (Ozerov et al., 2003). Our analysis is related to the non-linear analyses of chaotic processes, although in this study we base our conclusions on much more detailed observations of the chugging time series. Finally we present a new description of chugging events using wavelet transforms methods appropriate for non-stationary signals.

2. Data analysis

Eleven episodes of high signal–noise sequences of chugging were isolated at Sangay in the period of observation in 1998. These were extracted from the full data set and analyzed as described below. At least two sequences were complex series known as ‘intermittent chugging’ (Lees et al., 2004), i.e. sequences that were modulated by a much longer wavelength process, so those were broken down and investigated in parts. For each of the selected episodes, detailed analysis of the time intervals between individual chugs and the amplitudes of individual chugs was recorded (Fig. 2). To be as consistent as possible, automation of time and amplitude determinations was implemented. All time picks were made by selecting the maximum amplitude in a window surrounding each chug signal on the raw acoustic records. This approach eliminated the possibility of bias associated with decision making by an analyst. To provide estimates of the error in the automated picks, we used the following procedure: after arrival times were determined, a small window surrounding the maximum of each chug was selected and low-pass filtered using a Gaussian Nadaraya–Watson kernel regression smoother with central frequencies at 6 and 2 Hz respectively (R Development Core Team, 2006). The difference between the 2 Hz filtered maximum arrival-time/amplitude versus the 6 Hz arrival-time/amplitude represents an estimate of the quality of the arrival time

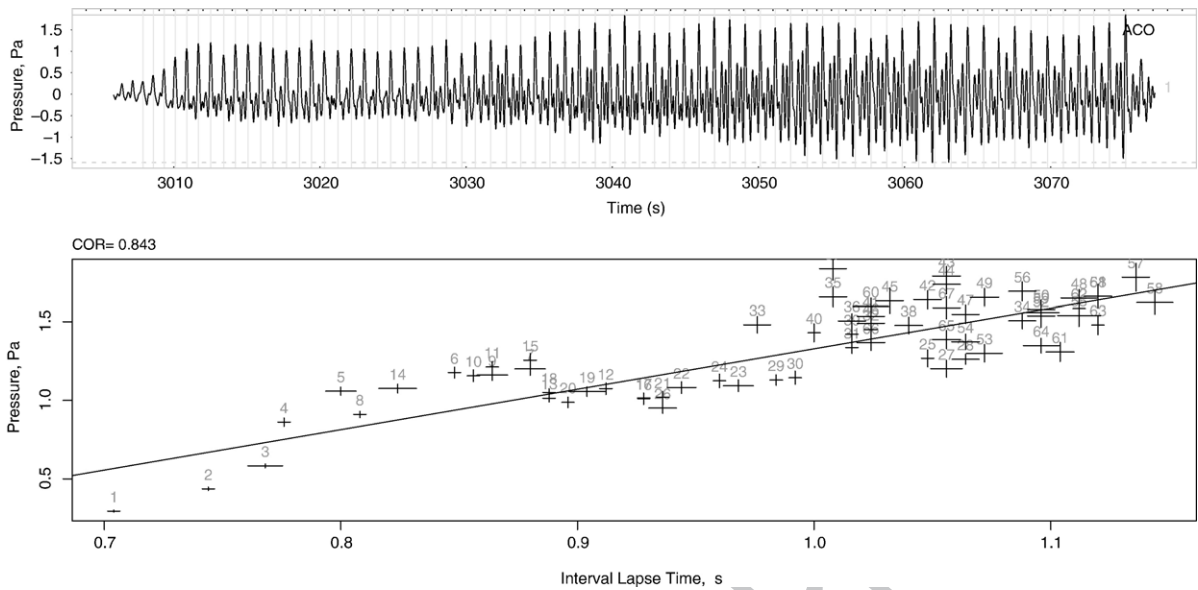


Fig. 2. Chugging Event #4. Each pulse is measured at its peak and errors of timing and amplitudes are estimated by comparing estimates with filtered versions of the pulses. Linear regression of time interval and amplitude is computed for each chugging sequence separately and error estimates are used to weight the linear models. The slope for Event 4 is 2.6 Pa/s with a correlation coefficient of 0.84. The number labels are the sequence of each pulse in the chugging series such that larger indices arrive later in time.

174 determination (Fig. 3). Uncertainty estimates rely on the
 175 choice of smoothing parameters, naturally, so an effort
 176 was made to design the filters that increase error bars
 177 when the peak region of the chug is multi-modal, or noisy.
 178 This method seemed to provide reasonable error bounds

in amplitude and time on the individual chugs, with
 179 maxima of 4.9% and 1.7% error variation, respectively.
 180
 181 The advantage of measuring time intervals so precisely
 182 over conventional spectrum methods is clear: estimates
 183 of frequency spectra generally mix signals over

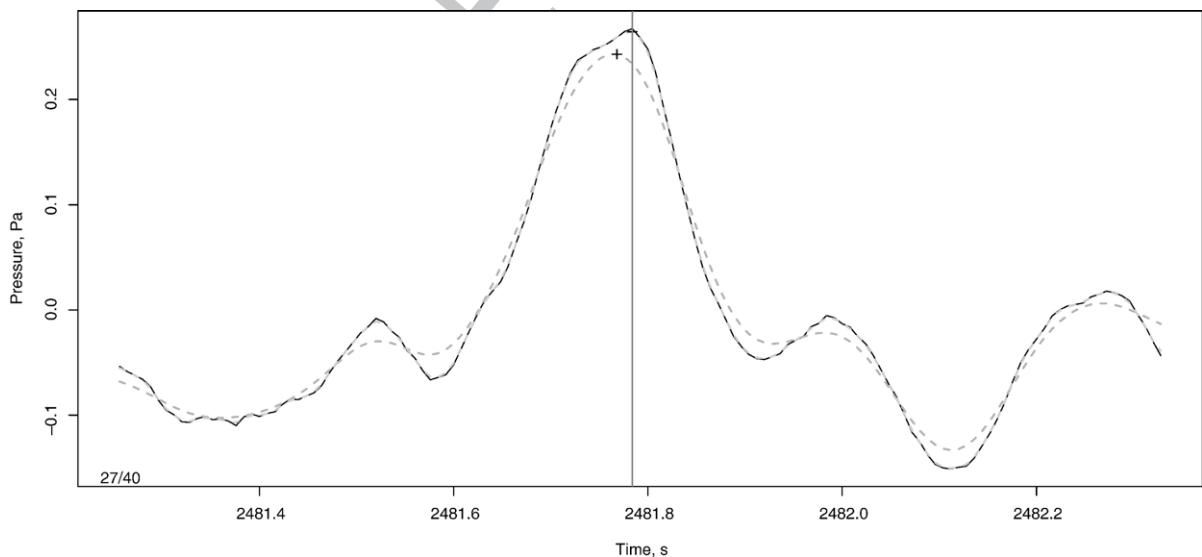


Fig. 3. Example chug illustrating estimates of error in time and amplitude. Arrival times are estimated by the peak amplitude in a short window surrounding the chug pulse. The pulse is smoothed at two different frequencies (dashed, grey lines) and the difference between the amplitude and arrival time of each (plus symbols) provides an automated method to extract the uncertainty of times and amplitudes. Uncertainties are used to weight the linear regression presented in Fig. 2.

184 several wavelengths to extract the frequency–amplitude
 185 information (Lees et al., 2004). The time-domain
 186 approach taken here preserves details of the structure of
 187 the sequence that cannot be obtained using a spectro-
 188 gram. The apparent relation between amplitude and time
 189 interval between chugs is further obscured by inconsis-
 190 tent estimation of the time arrivals, as would be the case if
 191 arrivals were determined by eyeball estimation. By devel-
 192 oping an automated algorithm to extract this informa-
 193 tion, the method can be applied to and compared with
 194 other datasets with general reliability.

195 3. Amplitude–time lapse analysis

196 We isolated eleven sequences of chugging activity
 197 and applied the automated time-domain analysis de-
 198 scribed above. Uncertainties in pulse arrival-time and
 199 amplitude estimates were used to weight linear regres-
 200 sions between lag (lapse) times and amplitudes. In nearly
 201 all the chugging sequences studied, there is a statistically
 202 significant positive correlation between amplitude and
 203 time interval between chugs (Fig. 4). While this ob-
 204 servation is not universal, i.e. there are sequences which
 205 do not show a strong correlation, in those instances

where chugging is relatively simple, the rule holds. 206
 Occasionally chugging sequences are complex, i.e. they 207
 are modulated by a longer period envelope that regulates 208
 amplitude fluctuations. In these cases, the chugging 209
 series were broken down and analyzed individually. The 210
 mean slope for sequences which had a statistically 211
 positive slope was 2.2 Pa/s. We note that accurate and 212
 stable calibration of the Venema electret microphone 213
 sensitivity is not available for data recorded at Sangay in 214
 1998 (Johnson et al., 2003). In this paper we used an 215
 estimated 30 mV/Pa to convert volts to pressure. The 216
 critical observation here is the positive relation between 217
 amplitudes and time lags whereas the absolute value of 218
 the slope is of lesser concern. 219

220 4. Frequency gliding

Frequency gliding occurs when the fundamental and 221
 corresponding harmonic frequencies fluctuate in time 222
 (Benoit and McNutt, 1997; Garces et al., 1998; Hagerty 223
 et al., 2000; Lees et al., 2004). At Langila volcano tremor 224
 related to puffing sounds of emissions exhibited frequen- 225
 cy variations greater than 50% over a time span of about 226
 1 min (Mori et al., 1989). The tremor at Langila had an 227

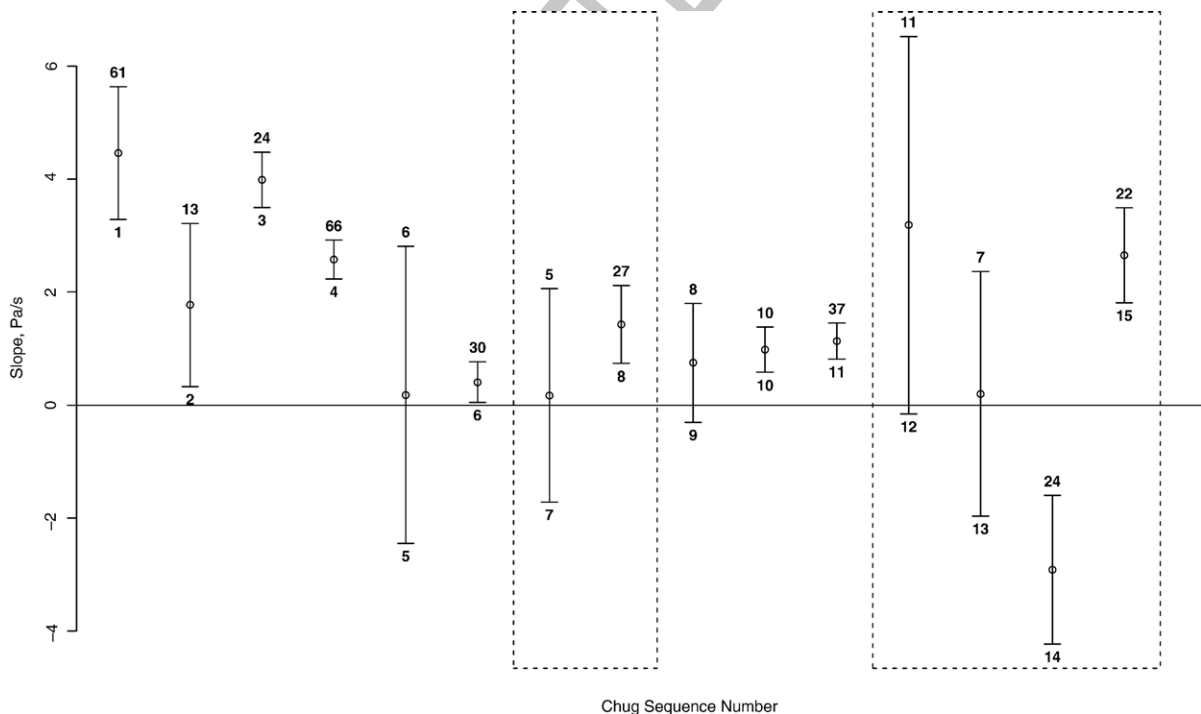


Fig. 4. Summary of regression analyses. Error bars are 95% confidence bounds formally estimated from linear regression. Each sequence is numbered (lower number) and shows the number of chugs per sequence (upper numeral). Sequence number 4 is presented in Fig. 2. Dashed boxes enclose sequences of intermittent chugging that were broken down into subsets and analyzed individually. The majority of chugging events at Sangay show a positive correlation between pulse interval time and amplitude.

228 increasing period for increasing amplitudes (Julian,
 229 1994). Frequency increments of about 100% over about
 230 10 min have been noted at Sakurajima volcano (Kamo
 231 et al., 1977). At Sangay we found that gliding often trends
 232 from higher to lower frequencies (Fig. 5), although
 233 occasionally chugging sequences appear to have the
 234 opposite trend. In some cases, however, gliding shows an
 235 increase and later a decrease in frequency over the time
 236 span of the sequence. Where chugging is interpreted as a
 237 superposition of standing waves, gliding has been viewed
 238 as a time varying change in the physical medium (for
 239 example, density fluctuations) which produce a drifting of
 240 the fundamental frequencies. Benoit and McNutt (1997)
 241 attributed frequency variations to changes in the dimen-
 242 sions of magma bodies or gas content. In linear oscillators,
 243 damping lowers the natural frequency of oscillation, in
 244 non-linear oscillators, damping can also have the opposite
 245 effect (Julian, 2000).

246 It has been established that volcano chugging cannot
 247 be modeled by a simple linear system of superposed
 248 oscillations (Lees et al., 2004). Since observations at
 249 Sangay appear to corroborate the conclusion that the
 250 underlying physical mechanism is non-linear, we propose
 251 that the observed frequency gliding is related to feedback
 252 loops in the vent-gas storage system near the opening of
 253 the conduit. As chugging progresses, the aperture where
 254 gasses are released undergoes slight modification,

255 coupled with fluctuations of internal pressures within
 256 the uppermost conduit. In nearly all cases where there was
 257 significant correlation between amplitude and interval
 258 time, higher amplitude pulses have longer times. This
 259 implies that the mechanism for releasing gasses is related
 260 to an increase of pressure associated with a larger volume
 261 of gas in the conduit chamber.

262 We found no correlation between isolated explosion
 263 event amplitude (non-chugging or chugging) and lapse
 264 time since the previous event. The physical mechanisms
 265 that control initial or isolated blasts are most likely dif-
 266 ferent from those governing chugging signals. During
 267 the 1998 field deployment, initial blasts at Sangay
 268 occurred once per hour, on average, producing hundreds
 269 of events (over this same period fewer than 20 sequences
 270 of chugging were observed, 11 of which are discussed
 271 here). All reports of activity from Sangay suggest that
 272 this activity has been ongoing since 1628 (Monzier et al.,
 273 1999). This is in marked contrast to Karymsky where
 274 Strombolian activity is intermittent with a decadal cycle
 275 that includes vigorous explosion cycles during the active
 276 phases. In spite of the differences in physical structure
 277 and geologic composition, the two volcano chugging
 278 sequences are remarkably similar in frequency content
 279 and amplitude range. We speculate that the physical
 280 processes governing all chugging signals is a feedback
 281 loop controlled by the geometry of the vent opening and

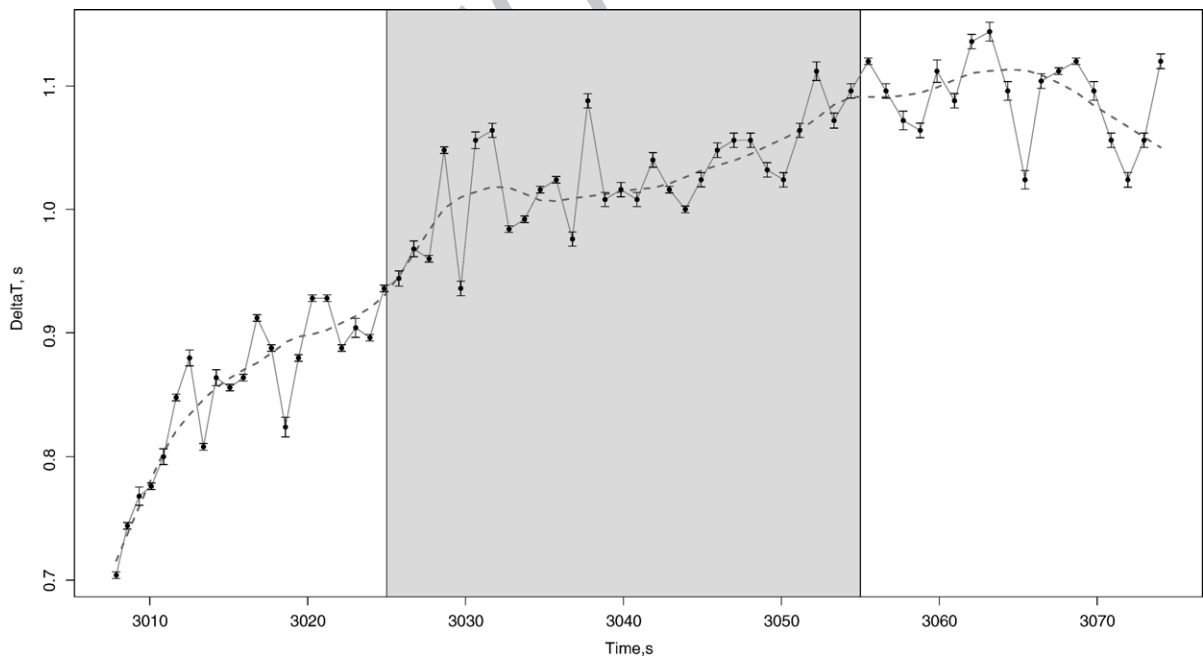


Fig. 5. Gliding interval time between chugs versus time from chugging sequence presented in Fig. 2. In this example the period between chugs increases, so the frequency decreases over the 60 s span of the chugging event. The shaded region corresponds to time periods discussed in the text where frequencies and particle motion vary. The dashed line is a smoothed representation of the points. Error bars for the timing are estimated as in Fig. 3.

282 the flux of gasses near the surface. For chugging at
 283 Karymsky and Sangay volcanoes parameters controlling
 284 gas flux appear to be similar. The vent at Karymsky
 285 during the times of observation was on the order of tens
 286 of meters with debris packing into the crater following
 287 each explosion. The aperture extent of the active vent at
 288 Sangay in 1998 is unknown because visual observations
 289 could not be made at that time. Gliding provides in-
 290 formation into the internal dynamics of the conduit
 291 physical state and we next invoke powerful processing
 292 tools to investigate it further.

293 5. Wavelet transforms

294 Application of the wavelet transform on the chugging
 295 sequence shown above reveals internal temporal varia-
 296 tion of the time history of the tremor. In this case we use
 297 the Morlet wavelet (Carmona et al., 1998; Addison,
 298 2002; Lees, 2005) as it is appropriate for Ricker type

wavelets often observed in seismic records. The mathe- 299
 matical form of the Morlet wavelet is a sinusoidal 300
 oscillation modulated by a Gaussian window function: 301

$$\psi\left(\frac{t-b}{a}\right) = \frac{1}{\pi^{1/4}} e^{i2\pi f_0[(t-b)/a]} e^{-\frac{1}{2}[(t-b)/a]^2} \quad (1)$$

where t is time, a is a scaling factor, b is shifting pa- 303
 rameter, f_0 is the center frequency for the wavelet, and i 304
 is the complex number. 305

An example wavelet transform is presented in Fig. 6 306
 with scale factor 1 and center frequency 5. The Morlet 307
 wavelet used in this study is designed so that the first two 308
 side lobes of the wavelet are approximately half the 309
 amplitude of the central peak (Carmona et al., 1998; 310
 Addison, 2002). We present the wavelet transforms of all 311
 four recorded signals, three seismic and one infrasound. 312
 Details of the wavelet transform of the infrasonic channel 313
 from Fig. 6 are presented in Figs. 7 and 8. 314

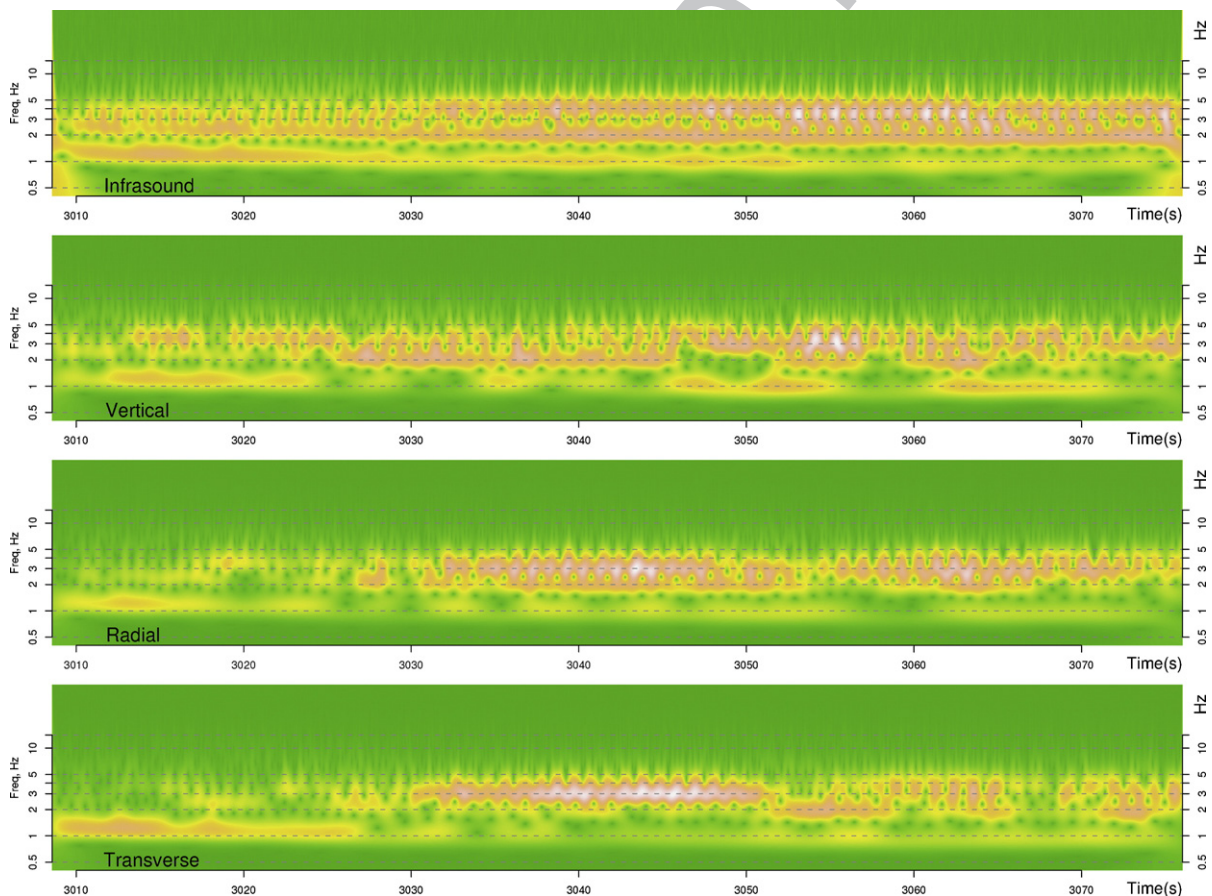


Fig. 6. Wavelet transform of chugging sequence #4. The figure shows all four channels: one infrasound and three-component seismic. The wavelet transform is designed to accentuate time varying frequency changes during the sequence of chugging tremor. The amplitude of the wavelet transform is based on a cross-correlation and has no units.

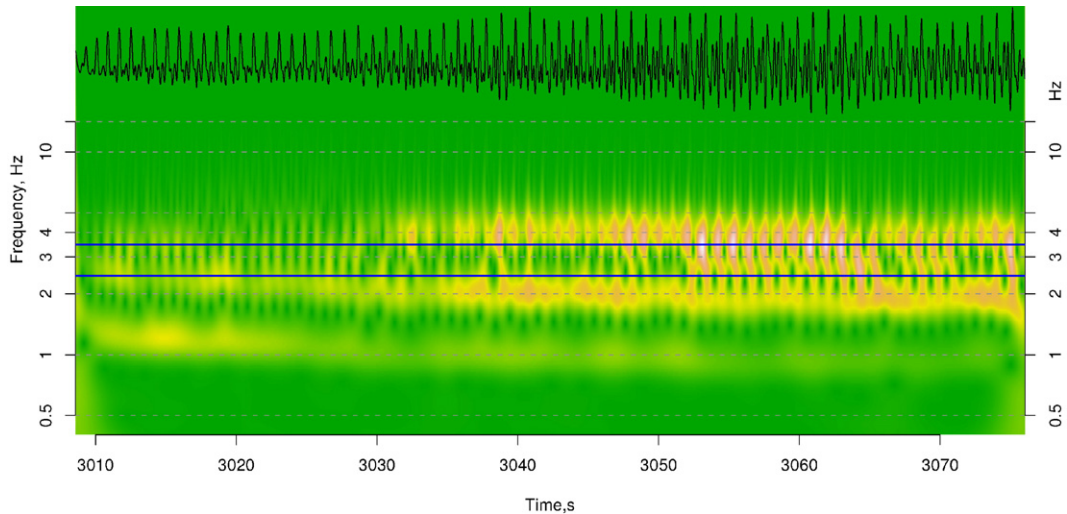


Fig. 7. Detail of wavelet transform of infrasonic component from Fig. 6. Two lines are drawn at frequencies 2.4 and 3.4 to illustrate the frequency-time varying behavior of the vent explosions during a chugging sequence. These rows are extracted in present in Fig. 8.

315 The wavelet transform can illuminate transient features in the signal that standard spectrograms, commonly
 316 used in seismology, do not show. In the example presented in Fig. 7 the wavelet transform accentuates
 317 individual pulses and relates information on how these pulses change with time and frequency. By focusing on
 318 details of the wavelet transform we can narrow down specific temporal variations in the chugging sequence.
 319 Consider two frequencies 3.4 Hz and 2.4 Hz in Fig. 7. Near time 3055 s there appears a slight bifurcation of the
 320
 321
 322
 323
 324

frequency content: pulses of 3.4 Hz are augmented by a
 325 series of 2.4 Hz wavelets. If we extract the rows of the
 326 wavelet transform at these frequencies (Fig. 8) the struc-
 327 ture become more apparent: around 3055 s the 2.4 Hz
 328 signal is time shifted relative the 3.4 Hz wave by about
 329 1.3 s, on average. This frequency time shift represents a
 330 new input at the source region where the infrasound
 331 pulses originate. Prior to 3055 the two frequencies are
 332 in phase, and then, rather abruptly, they are tuned out
 333 of phase. 334

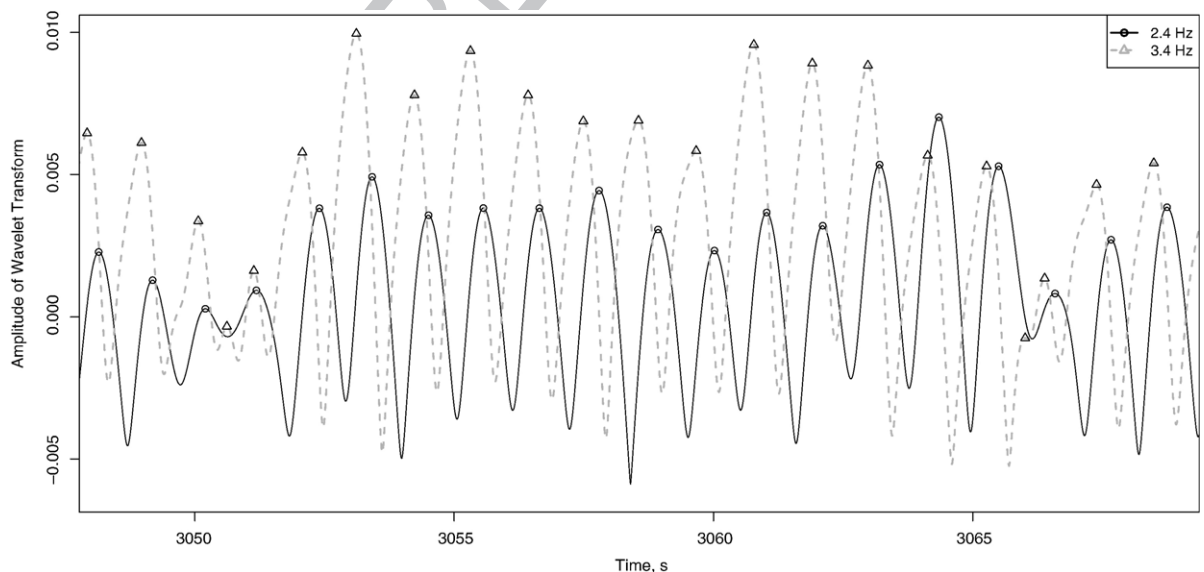


Fig. 8. Two rows of the infrasound wavelet transform extracted from Fig. 7 at 2.4 and 3.4 Hz. The marked peaks are measured in time and an average delay of 1.3 is estimated.

335 Analysis of particle motion during chugging se-
 336 quences is not commonly used, but in this case of
 337 chugging it reveals an interesting result. We speculate that
 338 particle motion orientation recorded at Sangay in 1998 is
 339 most heavily influenced by source effects rather than a
 340 path effects, i.e. waves arriving at the station are polarized
 341 at the source due to vent characteristics such as geometry,
 342 viscosity, or even directional and temporal source vari-
 343 ations which produce peculiar radiation patterns.

344 To analyze temporal variations in chugging particle
 345 motion, the three component seismic sequence is broken
 346 down into windows of 100 samples long (100/125 s) and
 347 eigenvectors of the point clusters for each window are
 348 calculated as the window migrates along the trace with
 349 75% overlap (Fig. 9, see (Lees, 2004) for a description of
 350 the methods). Measures of cluster quality are monitored
 351 along with the incident angle and azimuth of arrival. In
 352 this example (Fig. 9) there is good coherence in the initial
 353 part of the chugging sequence, during the first 20 s (time
 354 3000–3020 s), where the apparent motion of the particles
 355 at the seismometer is apparently 90° rotated from the

direction to the vent (Fig. 10). Then, at around 3025 s
 356 into the start of the sequence, a higher frequency wave
 357 arrives at the station and the particle motion shifts
 358 approximately 30° northward. We note that this effect is
 359 accompanied by a slight change in the acoustic signal,
 360 but a more significant change occurs at around time
 361 3055 s where lower frequencies appear to shift as il-
 362 lustrated in the previous paragraph (Figs. 7, 8, 9 and 10).
 363 It is clear that the dynamics of the chugging sequence
 364 varies over the time duration of the tremor, representing
 365 possible variations in explosion sources at the vent. The
 366 fact that the acoustic record changes in coordination with
 367 the seismic particle motion, suggests that particle motion
 368 variations originate at the source, since the acoustic
 369 waves do not share the same path effects as the seismic
 370 waves. A simple model consisting of superposition of
 371 standing waves in a column of rising magma or in a
 372 relatively shallow, mixed-phase conduit cannot explain
 373 these variations in behavior without invoking changes of
 374 the conduit geometry and/or physical characteristics
 375 over time periods of seconds or fractions thereof. On the
 376

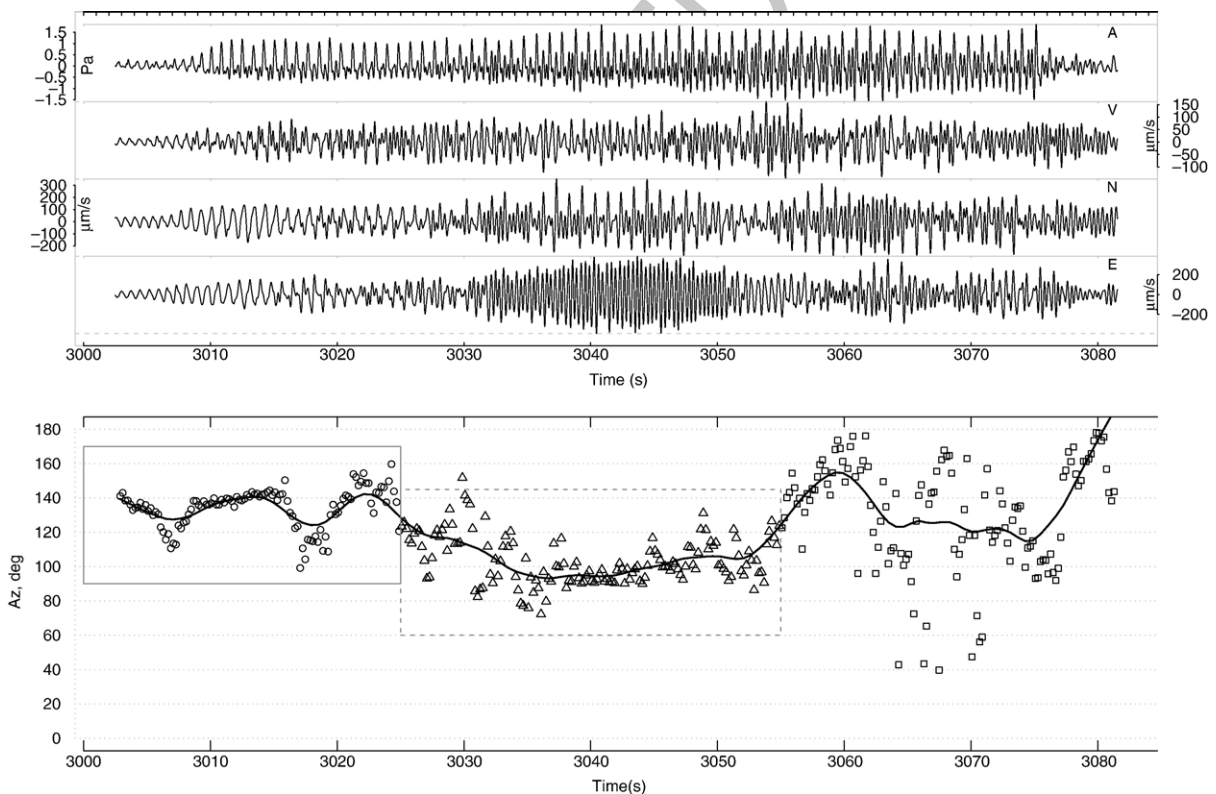


Fig. 9. Particle motion of chugging sequence. The upper panel shows the infrasound and the three components of the particle motion. The lower panel shows the azimuthal direction of particle motion estimated over moving windows of 100 samples (sample rate=0.008 s) with 75% overlap. The directions are derived from eigenvalue decomposition of velocity vectors, followed by projection onto the horizontal plane. The left box (3000–3025 s, circles) exhibits a significantly different orientation of particle motion than the central box. The central box (3025–3055 s, triangles) corresponds to the zone where the frequencies are shifting as described by the infrasound wavelet analysis.

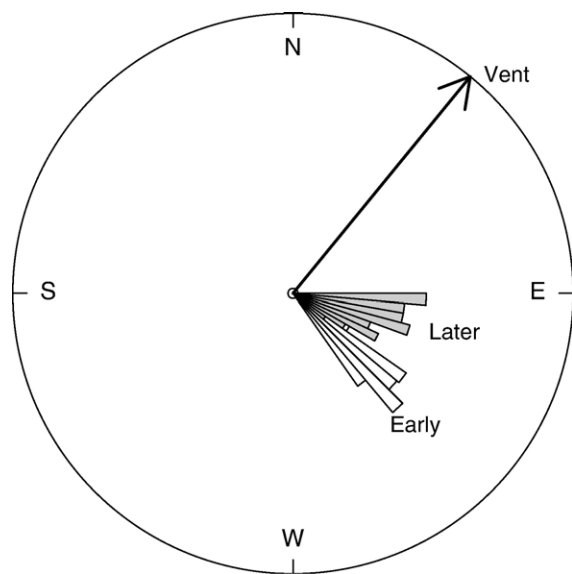


Fig. 10. Azimuthal distribution of particle motion relative to the vent direction. The “early” (white) period corresponds to time span 3000–3025 s (circles) in Fig. 9, the “later” (grey) period corresponds to time 3025–3055 s (triangles). A slight shift northward is seen in the orientation of the chugging signals over time corresponding to a change in explosion source orientation.

377 other hand if the extrusion of gases changes directions
 378 because of adjustments at the vent during the course of a
 379 chugging sequence, we may speculate that the shear
 380 waves arriving at the station rotate their orientation,
 381 producing the observed polarization shift.

382 6. Discussion

383 Lees et al. (2004) found a strong, apparently linear,
 384 correlation between chugging time intervals and corre-
 385 sponding signal amplitudes at Karymsky Volcano. Visual
 386 observations of Karymsky Volcano explosions in 1997/
 387 1998 suggest that, during chugging activity, Karymsky
 388 produced gas/ash explosions from a single eruption vent
 389 at the summit. The lone vent acted as the sole source of
 390 infrasonic activity, both for chugging and non-chugging
 391 events. Video recordings of explosions at Karymsky in
 392 1998 showed that at least two, distinct and separate
 393 plumes were evident during explosions (Johnson, in
 394 press). The plumes appeared to emanate from the same
 395 vent nearly simultaneously; a smaller, lighter colored
 396 cloud along with a darker, much larger plume of ash,
 397 pyroclastics and debris. We presume that the smaller,
 398 white plume consisted primarily of water vapor. During
 399 the 1998 deployment at Sangay, only one vent was
 400 observed and the presence or absence of multiple plumes
 401 is unknown.

Using a new technique in the time domain, a statis- 402
 tically significant positive correlation between time delays 403
 and pressure amplitudes of chugging events was found on 404
 Sangay’s infrasound data. This fact shows that chugging 405
 events at Karymsky and Sangay have more similarities 406
 than previously was noticed. The fact that amplitudes 407
 appear to be correlated with time intervals between chugs 408
 is significant. It suggests that it is highly unlikely that the 409
 process governing the chugging phenomenon can be 410
 modeled as a (simple, linear) superposition of waves in 411
 the conduit. This observation cannot be easily deduced 412
 from standard spectral analysis of the chugging se- 413
 quences. Frequency gliding has been observed at Arenal 414
 volcano, although the relation of amplitude to pulse 415
 frequency was not readily observed until it was noted at 416
 Karymsky (Lees et al., 2004). In this study we introduce 417
 the wavelet analysis to probe the time–frequency relation 418
 of the chugging sequences because standard spectrogram 419
 analysis smears information in time. The wavelet analysis 420
 has better time resolving power than traditional spectro- 421
 grams and thus shows details of frequency evolution. 422
 During the sequence where frequency splitting and abrupt 423
 changes occur over time spans of seconds (or less) the 424
 wavelet transform provides insight into time variations of 425
 the volcanic explosion source. 426

Konstantinou and Lin (2004) found that chugging 427
 signals from Sangay have a low correlation dimension 428
 (1.8–2.4) and a Lyapunov exponent in the range of 429
 0.013–0.022. From these results, they inferred that 430
 chugging events can be modeled by non-linear processes 431
 (positive Lyapunov exponent) with a low number of 432
 degrees of freedom given by a small fractal dimension. 433
 Theoretical process mechanisms can be generated by 434
 simple sets of non-linear, differential equations such as 435
 the Van der Pol or Duffing equations (Julian, 2000; 436
 Konstantinou and Schlindwein, 2003). While these 437
 equations retain some of the very gross characteristics 438
 of the tremor observed we have found simulations based 439
 on these simple assumptions seriously lacking. 440

A variety of non-linear, physical models have been 441
 postulated for harmonic tremor on Strombolian style 442
 explosive volcanoes, including: a) fluid flow through 443
 cracks (Julian, 1994, 2000); b) pressure cooker model 444
 (Lees and Bolton, 1998); and c) generation of Von 445
 Karman vortices related to obstructions in a conduit 446
 (Hellweg, 1999, 2000) and crack vibrations (Chouet, 447
 1986, 1988; Chouet et al., 2003). For now, we cannot 448
 speculate on the appropriateness of such models for 449
 illuminating the observations reported here, although it 450
 should be noted that it is possible to design sets of 451
 differential equations that produce sequences of signals 452
 similar to those discussed here. Lees and Bolton (1998) 453

proposed a set of non-linear differential equations relating choked flow with feedback mechanisms, although these models are still being explored to determine the best parameter estimates and their relation to physical volcanoes. Details of time series produced by these sequences of pulsations will have to be recorded with high fidelity at numerous stations before we can formulate reliable inverse procedures to determine the underlying physical processes. Furthermore, it is most probable that non-uniqueness of parameters sets defining small sets of differential equations proposed to simulate these phenomena will preclude a single, geologically significant, solution. Cross-disciplinary observations (thermal, visual, chemical, etc...) may offer hope to narrow model space of parameter sets that potentially satisfy the seismo-acoustic data, and some efforts along these lines are currently being investigated, although concrete results are not available as yet (Harris et al., 2003; Neuberg, 2006).

The correlation of particle motion variations and infrasonic frequency shifting suggests that the underlying geometry of the source is changing over the time span of one chugging event. At this point we do not have enough constraints to determine if changes in the source occur at depth (tens to hundreds of meters) or at the surface where the infrasound is generated. We speculate that it is unlikely that the variations observed here are produced by deep sources in the vent. Rather we suggest that perturbations shown above most probably result from rapid modifications of the near surface vent during the evolution of the chugging sequence. The modification maybe a slight opening or closing of the aperture or ablation of the edges of the vent which drives the frequency modulation and longer term gliding. A simple feedback mechanism that controls the pressure in the near surface conduit and the aperture of the vent can provide the necessary non-linear behavior required by the amplitude/repose time phenomena shown in Fig. 5. This model has been proposed by others (Johnson et al., 1998; Lees et al., 2004), although a strict mathematical formulation has not been worked out formally (Lees and Bolton, 1998).

7. Conclusions

By working in the time domain to estimate arrival times of pulses during tremor events we have reduced the error and increased the precision of time–amplitude observations of explosions at Sangay and Karymsky volcanoes. Sangay volcano exhibits quasi-periodic sequences of pulses following explosions which are known as chugging. Numerous sequences were analyzed and

shown to have a statistically significant positive correlation between amplitude and interval repose time. The strong correlation between pulse amplitude and repose time interval suggests feedback mechanisms and chaotic behavior similar to other volcanological phenomena where fluids are assumed to flow through narrow conduits and excite non-linear oscillatory vibration. The close association of particle motion variations and frequency-phase shifts estimated from wavelet transforms indicates modifications of the source/vent geometry rather than a deep seated variation. At the interface between the volcano and the atmosphere this phenomena leads to audible chugging that is prominent in the infrasonic bandwidth (0.7–2 Hz) and can be modeled as choked flow from a relatively shallow conduit chamber.

Acknowledgments

The authors thank Jeff Johnson for his help in collecting data at Sangay, and the IRIS PASSCAL instrument center for providing hardware and logistical support. This paper is dedicated to the memory of our friend Diego Viracucha who participated in the field deployment. The authors thank Vera Schindwein, editor Jeff Johnson, and an anonymous referee for constructive reviews. Support for this work was provided by grants NSF EAR 0337462 and NSF: EAR-9614639.

References

- Addison, P.S., 2002. The Illustrated Wavelet Transform Handbook: Introductory Theory and Applications in Science, Engineering, Medicine and Finance. Institute of Physics Publishing, Bristol. 353 pp.
- Benoit, J.P., McNutt, S.R., 1997. New constraints on source processes of volcanic tremor at Arenal Volcano, Costa Rica, using broadband seismic data. *Geophys. Res. Lett.* 24 (4), 449–452.
- Carmona, R., Hwang, W.-L., Torresani, B., 1998. Practical Time-Frequency Analysis: Gabor & Wavelet Transforms with an Implementation in S. Academic Press. 490 pp.
- Chouet, B., 1986. Dynamics of a fluid-driven crack in three dimensions by the finite difference method. *J. Geophys. Res.* 91, 13,967–13,992.
- Chouet, B., 1988. Resonance of a fluid-driven crack: radiation properties and implications for a source of long-period events and harmonic tremor. *J. Geophys. Res.* 93, 4375–4400.
- Chouet, B., et al., 2003. Source mechanisms of explosions at Stromboli Volcano, Italy, determined from moment-tensor inversions of very-long-period data. *J. Geophys. Res.* 2019. doi:10.1029/2002JB001919.
- Eichelberger, J.C., Izbekov, P.E., 2000. Eruption of andesite triggered by dyke injection: contrasting cases at Karymsky Volcano, Kamchatka and Mt. Katmai, Alaska. *Philos. Trans. R. Soc. Lond.* 358, 1465–1485.
- Garces, M.A., Hagerty, M.T., Schwartz, S.Y., 1998. Magma acoustics and time-varying melt properties at Arenal Volcano, Costa Rica. *Geophys. Res. Lett.* 25 (13), 2293–2296.
- Hagerty, M.T., Schwartz, S.Y., Garces, M.A., Protti, M., 2000. Analysis of seismic and acoustic observations at Arenal Volcano,

- 556 Costa Rica, 1995–1997. *J. Volcanol. Geotherm. Res.* 101 (1–2),
557 27–65.
- 558 Harris, A., et al., 2003. Ground-based infrared monitoring provides
559 new tool for remote tracking of volcanic activity. *Eos, Trans. - Am.*
560 *Geophys. Union* 84 (40), 409–418.
- 561 Hellweg, M., 1999. Listening carefully: unique observations of
562 harmonic tremor at Lascar volcano, Chile. *Annali di Geofisica*
563 42, 451–464.
- 564 Hellweg, M., 2000. Physical models for the source of Lascar’s harmonic
565 tremor. *J. Volcanol. Geotherm. Res.* 101 (1–2), 183–198.
- 566 Johnson, J.B., in press. On the relation between, infrasound,
567 seismicity, and small pyroclastic explosions at Karymsky Volcano.
Q3 568 *J. Geophys. Res.*
- 569 Johnson, J.B., Lees, J.M., 2000. Plugs and chugs — Strombolian
570 activity at Karymsky, Russia, and Sangay, Ecuador. *J. Volcanol.*
571 *Geotherm. Res.* 101, 67–82.
- 572 Johnson, J.B., Lees, J.M., Gordeev, E., 1998. Degassing explosions
573 at Karymsky Volcano, Kamchatka. *Geophys. Res. Lett.* 25 (21),
574 3999–4042.
- 575 Johnson, J.B., et al., 2003. Interpretation and utility of infrasonic
576 records from erupting volcanoes. *J. Volcanol. Geotherm. Res.* 121
577 (1–2), 15–63.
- 578 Julian, B.R., 1994. Volcanic tremor: nonlinear excitation by fluid flow.
579 *J. Geophys. Res.* 99 (B6), 11859–11877.
- 580 Julian, B.R., 2000. Period doubling and other nonlinear phenomena in
581 volcanic earthquakes and tremor. *J. Volcanol. Geotherm. Res.* 101
582 (1–2), 19–26.
- 583 Kamo, K., Furuzawa, T., Akamatsu, J., 1977. Some natures of volcanic
584 micro-tremors at the Skaura-jima volcano. *Bull. Vocanol. Soc. Jpn.*
585 22, 41–58.
- 586 Konstantinou, K.I., Schlindwein, V., 2003. Nature, wavefield properties
587 and source mechanism of volcanic tremor; a review. *J. Volcanol.*
588 *Geotherm. Res.* 119 (1–4), 161–187.
- 620 Konstantinou, K.I., Lin, C.H., 2004. Nonlinear time series analysis of
589 volcanic tremor events recorded at Sangay volcano, Ecuador. *Pure*
590 *Appl. Geophys.* 161 (1), 145–163. 591
- 592 Lees, J.M., 2004. Scattering from a fault interface in the Coso
593 geothermal field. *J. Volcanol. Geotherm. Res.* 130 (1–2), 61–75. 593
- 594 Lees, J.M., 2005. Wavelet transforms and volcanic explosions. *Eos,*
595 *Trans. AGU,* p. S31C-03. Fall Meet. Suppl. 595
- 596 Lees, J.M., Bolton, E.W., 1998. Pressure Cookers as Volcano Analogues.
597 *Eos, Trans. AGU,* p. 620. 597
- 598 Lees, J.M., Gordeev, E.I., Ripepe, M., 2004. Explosions and periodic
599 tremor at Karymsky Volcano, Kamchatka, Russia. *Geophys. J. Int.* 599
600 0 (0). doi:10.1111/j.1365-246X.2004.02239.x. 600
- 601 Monzier, M., et al., 1999. Sangay Volcano, Ecuador; structural
602 development, present activity and petrology. *J. Volcanol. Geotherm.*
603 *Res.* 90 (1–2), 49–79. 603
- 604 Mori, J., et al., 1989. Seismicity associated with eruptive activity at
605 Langila volcano, Papua New Guinea. *J. Volcanol. Geotherm. Res.* 605
606 38, 243–255. 606
- 607 Neuberg, J.W., 2006. Multi-parameter monitoring and modelling of
608 volcanic processes. In: Mader, H.M., Coles, S.G., Connor, C.B.
609 (Eds.), *Statistics in Volcanology*. Special Publications of IAVCEI.
610 Geological Society, London, pp. 215–230. 610
- 611 Ozerov, A., Ispolatov, I., Lees, J., 2003. Modeling Strombolian eruptions
612 of Karymsky volcano, Kamchatka, Russia. *J. Volcanol. Geotherm.*
613 *Res.* 122 (3–4), 265–280. 613
- 614 R Development Core Team, 2006. R: A Language and Environment for
615 Statistical Computing. In: R.F.f.S.Computing (Ed.), Vienna, Austria. 615
- 616 Zobin, V.M., Levina, V.I., 1998. Rupture history of the January 1,
617 1996, Ms 6.6 volcanic earthquake preceding the simultaneous
618 eruption of Karymsky and Akademia Nauk volcanoes in
619 Kamchatka, Russia. *J. Geophys. Res.* 103 (8), 18,315–18,324. 619